AIIM

Association for Information and Image Management

1100 Wayne Avenue, Suite 1100
Silver Spring, Maryland 20910
301/587-8202

Centimeter

Inches

MANUFACTURED TO AIIM STANDARDS
BY APPLIED IMAGE, INC.

PNL-SA-24063

A STRATIFORM CLOUD PARAMETERIZATION FOR GENERAL CIRCULATION MODELS

S. J. Ghan
L. R. Leung
C. C. Chuang[a]
J. E. Penner[a]
J. McCaa[b]

February - March 1994

Presented at the
Atmospheric Radiation Measurement
Science Team Meeting
February 28 - March 3, 1994
Charleston, South Carolina

Work supported by
the U.S. Department of Energy
under Contract DE-AC06-76RLO 1830

Pacific Northwest Laboratory
Richland, Washington 99352

(a) Lawrence Livermore National Laboratory
Livermore, California
(b) University of Washington
Seattle, Washington

CONF-940277--1

A Stratiform Cloud Parameterization for General Circulation Models

Steven J. Ghan and L. Ruby Leung, Pacific Northwest Laboratory
Catherine C. Chuang and Joyce E. Penner, Lawrence Livermore National Laboratory
James McCaa, University of Washington

The crude treatment of clouds in General Circulation Models (GCMs) is widely recognized as a major limitation in the application of these models to predictions of global climate change. The purpose of this project is to develop a parameterization for stratiform clouds in GCMs that expresses stratiform clouds in terms of bulk microphysical properties and their subgrid variability. In this parameterization, precipitating cloud species are distinguished from non-precipitating species, and the liquid phase is distinguished from the ice phase. The size of the non-precipitating cloud particles (which influences both the cloud radiative properties and the conversion of non-precipitating cloud species to precipitating species) is determined by predicting both the mass and number concentrations of each species.

Cloud Microphysics

The stratiform cloud parameterization is based on a bulk cloud microphysics parameterization originally developed at Colorado State University for mesoscale cloud models (Tripoli and Cotton, 1980; Cotton et al., 1982; Cotton et al., 1986; Meyers et al., 1992). We first improved the computational efficiency of the parameterization by introducing two approximations appropriate for stratiform clouds (Ghan and Easter, 1992), so that the parameterization can now be applied to GCMs.

To permit application to both polluted continental clouds and pristine marine clouds, we have introduced the droplet number concentration N_c as a prognostic variable:

$$\frac{\partial N_c}{\partial t} = -\nabla \cdot (N_c \mathbf{V}) + NU_{vc} - N_c[CN_{cr} + CL_{cr} + CL_{ci} + CL_{cs} + FR_{ci}]/r_c \qquad (1)$$

Here $\mathbf{V}$ is three-dimensional velocity, NU_{vc} the rate of droplet nucleation, CN_{cr} the rate of autoconversion of cloud droplets to rain, CL_{cr}, CL_{ci}, and CL_{cs} the rates of collection of cloud droplets by rain, ice and snow, respectively, FR_{ci} is the rate of freezing of supercooled cloud droplets to form cloud ice, and r_c is cloud water mass concentration.

Most of the sink terms in the droplet number balance follow from the sink terms in the cloud water mass concentration, assuming the sink processes affect the cloud water mass and

and number concentration, but not the average droplet mass. The droplet number sink due to autoconversion of cloud water to rain is parameterized according to Ziegler (1985).

The droplet source reflects the nucleation of cloud droplets when aerosols are activated as cloud condensation nuclei. If we assume droplets are formed only as air enters a cloud, then the droplet source can be expressed

$$NU_{vc} = -\nabla \cdot (N\mathbf{V}) \tag{2}$$

where N is zero except for inflow on the cloud boundaries, when it equals the number concentration of aerosols activated. The droplet source term represents a flux convergence of droplets into the cloud, which is not accounted for by the transport term $\nabla \cdot (N_c\mathbf{V})$ because the treatment of transport assumes no droplets flow into the cloud.

We have found that, in applying (2) to the prognostic equation for droplet number, turbulent variations in velocity V must be considered if the prognostic equation for droplet number also includes a treatment of turbulent transport that, like the treatment of resolved transport, assumes no droplets flow into the cloud. Such a treatment is consistent with the inhomogeneous model of droplet evaporation due to mixing (Baker and Latham, 1979). Thus, if the turbulent transport is expressed in terms of a vertical diffusivity K, the droplet nucleation term for a layer at the base of a Euclidian (rectangular) stratiform cloud can be written

$$NU_{vc} = \frac{[\max(w_b, 0) + \frac{K_b}{\Delta z}]N_b}{\Delta z} \tag{3}$$

where w is the vertical velocity, Δz is the model layer thickness, and the subscript b denotes cloud base. Note that we neglect droplet nucleation on the sides of the clouds.

To determine the number concentration of droplets nucleated, N_n, we have developed a parameterization in terms of the vertical velocity and the aerosol number concentration, N_a:

$$N_n = \frac{w^* N_a}{w^* + cN_a} \tag{4}$$

where c is a coefficient that depends on the temperature, pressure, aerosol composition and the mode radius and standard deviation of the aerosol size distribution (Ghan et al., 1993), and

$$w^* \equiv w + \frac{\alpha}{\alpha + \beta}\left[\frac{c_p}{g}\frac{T}{\theta}\frac{1}{\rho}\nabla \cdot \rho\overline{\theta'\mathbf{V}'} - \frac{Q_r}{g} - \frac{q_s}{\alpha}\frac{c_p}{g}\frac{1}{\rho}\nabla \cdot \rho\overline{q_v{'}\mathbf{V}'}\right] \tag{5}$$

with $\alpha \equiv \frac{\partial q_s}{\partial T}$, $\beta \equiv \rho c_p \frac{\partial q_s}{\partial p}$, and Q_r the radiative heating rate (Ghan et al., 1993). Note that with the general expression (5) the parameterization accounts for supersaturation forcing by radiative cooling, turbulence moistening, and turbulent cooling. We have compared the number nucleated according to (4) with that simulated by a detailed size-resolving nucleation model (Edwards and Penner, 1988), and have found that, even for realistic aerosol size distributions, the number nucleated agrees to within 30% for vertical velocities ranging from 1 to 500 cm $s^{-1}$and aerosol number concentrations ranging from 50 to 5000 cm^{-3} .

The parameterization (4) is restricted to the case of a single aerosol type. We have now developed a parameterization applicable to the more general case of activation of multiple aerosol types, with different compositions or size distributions. The different aerosol types can compete with each other as cloud condensation nuclei. Figure 1 compares the parameterized and simulated number fraction of aerosols activated for each of two competing aerosol types. The number concentrations and size distributions of both aerosol types are identical, but type one aerosol is fully soluble while type two aerosol is composed of 10% soluble material. The parameterization correctly predicts the more efficient activation of the more soluble aerosol type, with errors in the fraction activated between 20 and 50%. Additional comparisons are reported in Ghan et al. (1994).

Subgrid Cloud Parameterization

Sub-grid scale variations in cloud microphysical processes must be accounted for in GCMs because cloud processes are highly nonlinear and are poorly resolved by the coarse grid size of GCMs. We express subgrid variations in cloud properties in terms of idealized probability distributions of the cloud variables. We assume most subgrid variability in stratiform clouds is due to turbulence, and use the Mellor-Yamada second-order turbulence closure scheme to predict the variance of cloud variables. We account for subgrid cloud variations in cloud processes by integrating the expressions for the cloud processes over the probability distributions of the cloud variables. For example, the flux of cloud droplets at cloud base is expressed

$$\overline{w'N'} = \int_0^\infty wNP(w)dw \tag{6}$$

where $P(w)$ is the probability distribution of vertical velocity, determined from the predicted mean and variance of vertical velocity.

Application to a Single Column Model

To test the subgrid cloud parameterization, we have applied it to a single column model. In addition to cloud microphysics and turbulence, the model treats vertical advection, radiative transfer and surface processes. Figure 2 illustrates a simulation of a boundary layer cloud driven only by radiative cooling. The subgrid standard deviation in cloud water is greatest near cloud top, where strong radiative cooling drives turbulent mixing, but is much smaller than the mean cloud water at all levels. The cloud fraction is consequently unity throughout the depth of the cloud. With droplet number concentration prescribed at 300 cm^{-3} , no precipitation forms because subgrid variability in autoconversion is not yet treated.

Application to a GCM

We have applied the bulk cloud microphysics parameterization to the PNL version of the NCAR CCM. We have replaced the usual prognostic variables temperature T and water vapor mixing ratio r_v with the condensation-conserved variables $T_{cld} = T - L/c_p r_c$ and $r_w = r_v + r_c$, where L is the latent heat of condensation. Temperature, water vapor, and the cloud water mixing ratio r_c can be diagnosed from T_{cld} and r_w by assuming condensation instantaneously eliminates supersaturations with respect to liquid water. Advection of cloud water is implicitly treated in the advection of T_{cld} and r_w, and therefore need not be treated explicitly, thus eliminating problems associated with advecting a field with frequent zeroes. Subgrid variations in stratiform clouds are not yet treated, but detrainment of condensed water from cumulus clouds is. We have performed one preliminary thirty-day simulation with prescribed droplet number and have found that, without any tuning, the simulated global planetary radiation balance is within 10 W m^{-2} of satellite observations for both solar and infrared radiation (Table 1). Figure 3 shows the latitudinal distributions of zonal mean simulated and observed planetary radiation balance. Simulated cloud cover is high, about 80%, because the model simulates extensive ice clouds that are too thin to be observed.

References

Baker and Latham, 1979: The evolution of droplet spectra and the rate of production of embryonic raindrops in small cumulus clouds. J. Atmos. Sci., 36, 1612-1615.

Cotton, W. R., M. A. Stephens, T. Nehrkorn and G. J. Tripoli. 1982. The Colorado State University Three-Dimensional Cloud/Mesoscale Model. Part II: An Ice Phase Parameterization. J. Rech. Atmos. 16:295-320.

Cotton, W. R., G. J. Tripoli, R. M. Rauber, and E. A. Mulvihill. 1986. Numerical

Simulation of the Effects of Varying Ice Crystal Nucleation Rates and Aggregation Processses on Orographic Snowfall. J. Clim. Appl. Meteor. 25:1658-1680.

Edwards, L., and J. E. Penner. 1988. Potential Nucleation Scavenging of Smoke Particles Over Large Fires: A Parametric Study. In Aerosols and Climate, eds. P. V. Hobbs and M. P. McCormick. A. Deepak Publishing, pp. 423-434.

Ghan, S.J., and R.C. Easter, 1992. Computationally Efficient Approximations to Stratiform Cloud Parameterization. Monthly Weather Review, 120:1572-1582.

Ghan, S.J., C.C. Chuang, and J.E. Penner. 1993. A Parameterization of Cloud Droplet Nucleation, Part I: Single Aerosol Type. Atmospheric Research, 30, 197-221.

Ghan, S.J., C.C. Chuang, R.C. Easter, and J.E. Penner, 1994: A parameterization of cloud droplet nucleation. Part II: Multiple aerosol types. Atmospheric Research, in press.

Meyers, M.P., P.J. DeMott, and W.R. Cotton. 1992. New Primary Ice Nucleation Parameterizations in an Explicit Cloud Model. J. Appl. Meteor., 31:708-721.

Tripoli, G. J., and W. R. Cotton. 1980. A Numerical Investigation of Several Factors Contributing to the Observed Variable Intensity of Deep Convection over South Florida. J. Appl. Meteor. 19:1037-1063.

Ziegler, C.L., 1985: Retrieval of thermal microphysical variables in observed convective storms. Part 1: Model development and preliminary testing. J. Atmos. Sci., 42, 1487-1509.

Table 1. Planetary Radiation Balance (July)

	Simulated $W\ m^{-2}$	Observed $W\ m^{-2}$
Outgoing Longwave		
clear-sky	269	268
total	228	238
cloud forcing	41	30
Absorbed Solar		
clear-sky	284	281
total	240	234
cloud forcing	-45	-46
Net ERB		
clear-sky	15.3	13.5
total	11.5	-3.1
cloud forcing	-3.8	-16.6

Figure Captions

Figure 1. Number fraction of aerosols activated for two competeing aerosol types, as simulated (asterisks) and as parameterized (solid line), plotted as functions of the updraft velocity. One aerosol type (left) is fully soluble, while the fraction of soluble material of the other (right) is 10%.

Figure 2. Mean cloud water (solid line) and standard deviation of cloud water (dashed line) as functions of altitude for a stratocumulus cloud driven by radiative cooling.

Figure 3. Zonal mean planetary albedo (left) and outgoing longwave radiation (right) as simulated by the PNL version of the NCAR CCM1 (solid line) and as observed by the Earth Radiation Budget Satellite (dashed line) for July.

/.

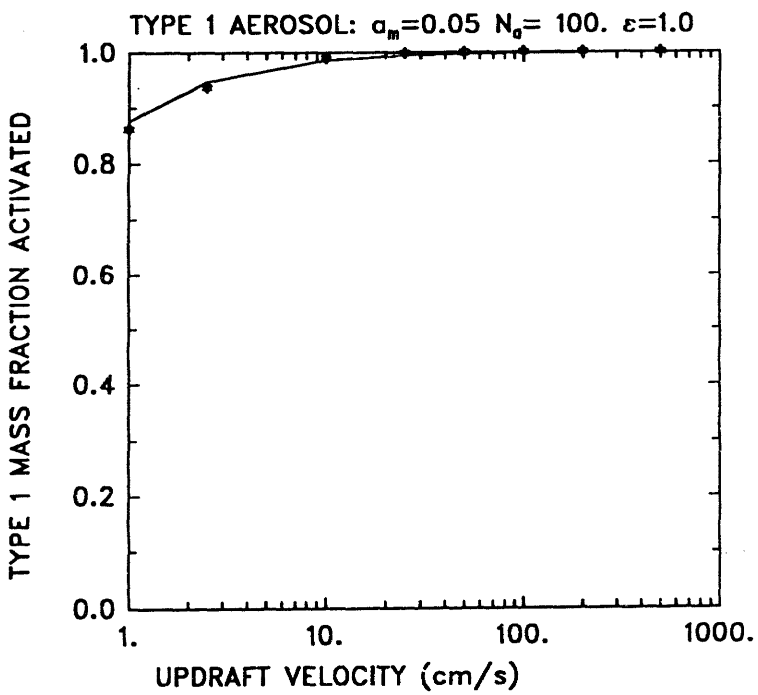
TYPE 1 AEROSOL: a_m=0.05 N_a= 100. ε=1.0
TYPE 1 MASS FRACTION ACTIVATED
UPDRAFT VELOCITY (cm/s)
0.0
0.2
0.4
0.6
0.8
1.0
1.
10.
100.
1000.

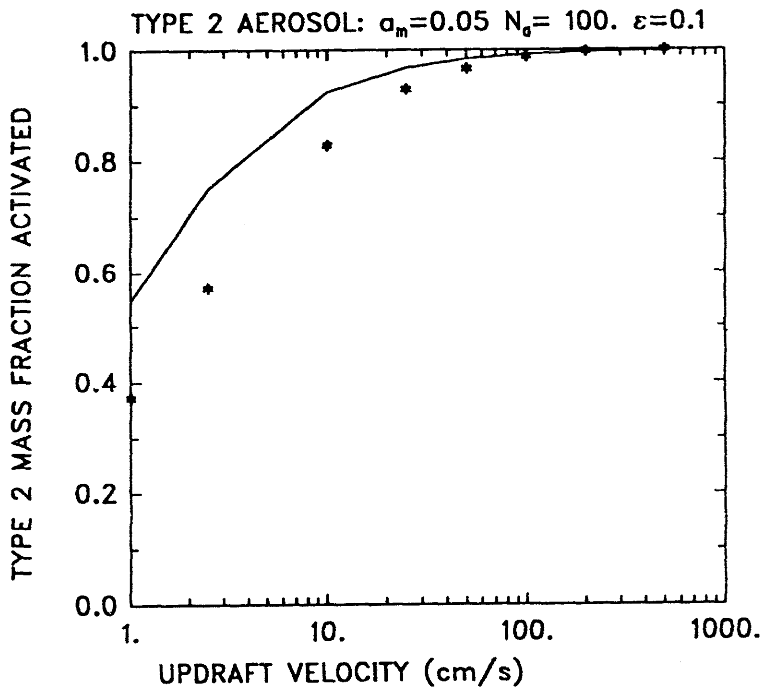
TYPE 2 AEROSOL: a_m=0.05 N_a= 100. ε=0.1
TYPE 2 MASS FRACTION ACTIVATED
UPDRAFT VELOCITY (cm/s)
0.0
0.2
0.4
0.6
0.8
1.0
1.
10.
100.
1000.

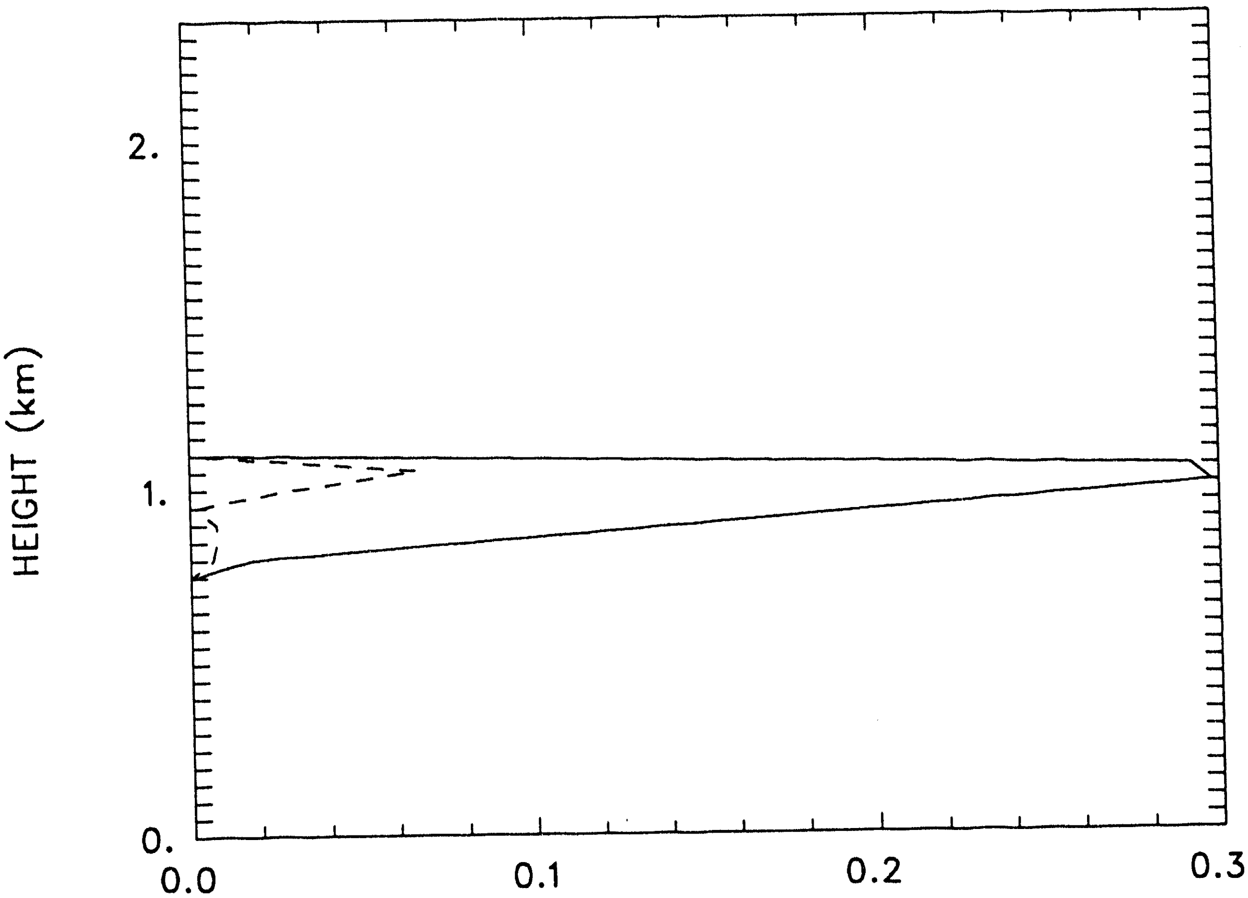

HEIGHT (km)
2.
1.
0.
0.0
0.1
0.2
0.3

3.

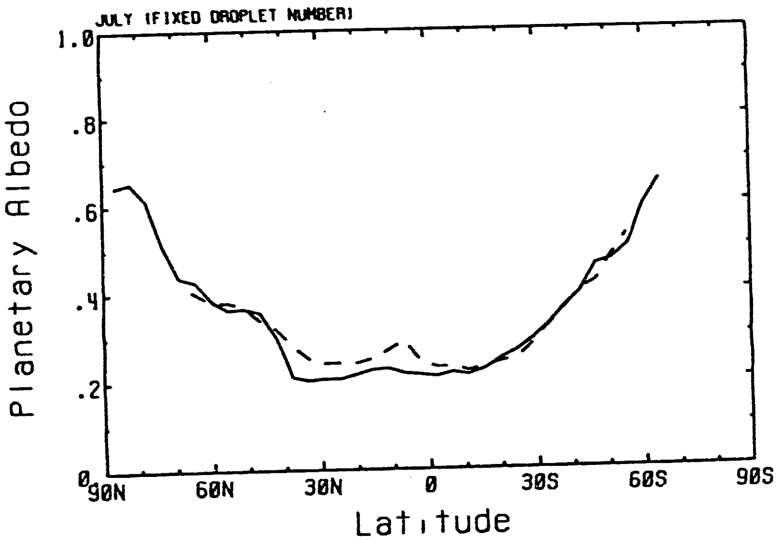

Outgoing Longwave Radiation